
S-Flow GAN

Yakov Miron , Yona Coscas
 Elbit Systems Aerospace
 {yakov.miron, yona.coscas}@elbitsystems.com

Abstract

This work offers a new method for generating photo-realistic images from semantic label maps and a simulator edge map images. We do so in a conditional manner, where we train a Generative Adversarial network (GAN) given an image and its semantic label map to output a photo-realistic version of that scene. Existing architectures of GANs still lack the photo-realism capabilities. We address this issue by embedding edge maps, and presenting the Generator with an edge map image as a prior, which enables generating high level details in the image. We offer a model that uses this generator to create visually appealing videos as well, when a sequence of images is given.

1 Introduction

The topic of image to image translation and more generally video to video translation is of major importance for training autonomous systems. It is not practical to train an agent’s neural network (NN) in real environments, since sufficient reliability cannot be achieved using real images taken by the agent in real environments. Self-driving car for example cannot gather enough data in real environments to achieve the required reliability [6]. Moreover, using simulated scenes for training might lack details since a synthetic image will not be photo-realistic and lack the variability and randomness of real images, causing training to succeed up to a certain point. This gap is also referred to as “the reality gap” [6]. By combining a non photo-realistic, simulated model with an available dataset, we can generate diverse scenes containing numerous types of objects, lightning conditions, colorization etc. [5].

In this paper, we depict a new approach to generate images from a semantic label maps and a flexible Deep Convolutional Neural Network (DCNN) we called Deep Neural Edge Detector (DNED) which embed an edge map. When taking images from a simulated scene, one can use the available semantics given by the simulator engine. This semantic map, combined with an edge map, generated by the simulated images and embedded by a DNED, is the input to our model (fig 1), The model outputs a photo-realistic version of that scene. We have extended this idea to generate photo-realistic videos (i.e. sequence of images) with a new, simple loss. To generate coherent images and visually appealing videos, we estimate and incorporate a temporal flow map on consecutive images.

Recent works in the field of image generation include pix2pix [17] offering image generation from semantic maps, cascaded refinement networks [5] generating photographic images using cascaded refinement networks, pix2pixHD [35] can generate HD images in a conditional manner using multi-scale discriminator and an external generator architecture. L1 loss for image generation is known to generate low quality images as the generated images are blurred and lack details [9]. Instead, [10], [18] are using a modified version of the perceptual loss, allowing generation of finer details in an image. Pix2pixHD [35] and CRN [5] are using a perceptual loss as well for training their networks, e.g. VGGnet [29]. Moreover, pix2pixHD are using the instance maps in addition to the label maps to provide the generator with the ability to separate several objects of the same semantics. This is of



Figure 1: in this paper we propose a method for generating photo-realistic images from semantic labels of a simulator scene. This figure provides images related to the Synthia dataset [24]. Left - semantic map of the scene. Middle - generated image from pix2pixHD [35]. Right - Our generated image. The texture and color space in our generated image is more natural giving the image the desired photo-realism.

high importance when synthesizing images having many instances of the same semantics in a single frame.

As for video generation the loss used by [34], [28] tend to be computationally expensive while our approach is simpler. In our approach, we are using two generators of the same architecture, where one drives the other and they are trained jointly using our new Flow loss. Since our main objective is generating photo-realistic images and appealing videos from simulated ones, and following Blau [4], that depicts the perception-distortion tradeoff, we were not seeking quantitative results, but qualitative ones, therefore well known scores like PSNR, SSIM, etc. were not used for comparison. We call this work s-Flow GAN since we embed Spatial information in a neural network as a prior for image generation and flow maps for video coherency.

We make Three major contributions: First, our model can generate visually appealing photo-realistic images. Second, we incorporate a neural network to embed edge maps, thus allowing generation of diverse versions of those generated images. Third, we offer a new and simple loss function for generating natural looking videos using the above mentioned generator.

2 Related Work

2.1 Generative Adversarial Networks

Generative Adversarial Networks (GAN) were introduced in 2014 [12]. This method can generate images that look authentic to human observers. They do so by having two neural networks, where one generates candidates while the other acts as a critique and tries to evaluate the generation quality [2],[23],[40],[41],[26]. GANs are widely used for image generation; most image synthesis schemes are used to generate low resolution images e.g. 32x32 [17] while the one able to generate high resolution images use coarse-to-fine generators [35], the reason for that limitation is the high dimensionality of the image generation task and the need to provide queues for high resolution [22], [19]. In our work, we suggest an architecture to embed edge map queues in the DNED module. During training the DNED is trained to learn the representations of real image edge maps. During test the DNED is shown a CG (Computer Graphics) edge map, finds its best representation and provides the generator with an appropriate generated edge map sampled from real image edge maps distribution.

2.2 Image to image translation

In the pix2pix setting, they used a Conditional GAN [21], where the network’s input is a semantic map of the scene, and while training in adversarial mode, a fake version of the real image is given to the discriminator to distinguish. In our setting e.g. CG2real, in addition to the semantic map we also have access to the simulated image. Using the CG image as an input to the network is usually counter productive since it will be trained to reconstruct CG images and not photo-realistic ones. Conversely some of the underlying CG information correlates with the real world and can provide meaningful prior to the synthesis. Since the relevant information lies in high resolution details, which is also the drawback of GANs, we suggest learning the distribution of edge maps (high resolution details) in real semantic labels, and providing it to the generator at test time.



Figure 2: example of the images for training the model. Left is the semantic map. Middle is the edge map extracted from the real image. Right is the real image being used by the discriminator for adversarial training. Please note that the real image is not used by the generator neither at training nor at test time, but only its edge map. The main issue in the CG2real model compared to the image to image models is that the simulator’s image is available to the generator at test time. We thus use the simulator’s image to extract the edge map allowing the generator to generate the necessary fine details in the output image.

2.3 Learning edges by a neural network

Generating edge maps using neural networks is a well established method. Holistically-Nested Edge Detection (HED) provides holistic image training and prediction for multi-scale and multi-level feature learning [37]. They use a composition of generated edge maps to learn a fine description of the edge scene. Inspired by their work, we train a neural network to learn edge maps of the real image.

We train a DCNN to generate edge maps and provide it as a prior to the generator, which guides it in the image synthesis process. The reason we use a DCNN to learn the edge maps instead of using the edge map operator, e.g. Laplacian, is to allow the variability of fine details in our model. If a deterministic edge map was used, we would generate a single image in a CG2real setting. By using a DCNN, we allow it to embed all the semantic edge maps provided at training thus creating diverse scenes from the same input.

Some image generation tasks use label maps only, e.g. [17]. The label maps provide only information about the class of a given pixel. In order to generate photo-realistic images, some use instance maps as well [35]. This way, they can differentiate several adjacent objects of the same class. Nonetheless, while most datasets provide object level information about classes like cars, pedestrians, etc. they do not provide that information about vegetation and buildings. As a result, the generated images might not correctly separate those adjacent objects, thus degrading photo-realism. Our approach which incorporates edge maps, can mitigate this issue since edge maps are not class dependent, thus contain the desired fine details separation of objects, and achieve instance level performance only using label maps as can be seen in fig 3.2.

2.4 Video to video synthesis

Generating temporally coherent image sequences is a known challenge. Recent works use GANs to generate videos in an unconditional setting [25],[31],[33], by sampling from a random vector, but don’t provide the generator with temporal constraints, thus generating non coherent sequences of images. Other works like video matting [3] and video inpainting [36] translate videos to videos but rely on problem specific constraints and designs. A recent work named vid2vid [34] offers to conditionally generate video from video and is considered to one of the best approaches to date. Using FlowNet 2.0 [16] they predict the optical flow of the next image. In addition, they use a mask to differentiate between two parts; the hallucinated image that is generated from instance-level semantic segmentation masks and the predicted image from the previous frame. By adding these two parts, this method can combine the predicted details from the previously generated image, with the details from the newly generated image. Inspired by [34], we are using flow maps of consecutive images to generate temporally coherent videos. Contrary to [34] we are not using a DCNN to predict the flow maps or a sequence generator, thus enabling better temporal coherency and image quality. Instead we incorporate flow maps in a new and simple loss function as will be depicted below.

3 Model

Our CG2real model aims to learn the conditional distribution of an image given a semantic map. Our video generation model aims to use this learned distribution for generating temporally coherent videos using the generated images from the CG2real scheme. We first depict the image generation scheme, then we review our video generation model.

3.1 Image generation

We use a conditional GAN to generate images from semantic maps as in [17]. In order to generate images, the generator receives the semantic segmentation images s_i and maps it to photo-realistic images x_i . In parallel, the discriminator takes two images, The real image x_i (ground truth) and the generated image f_i and learns to distinguish between them. This supervised learning scheme is trained in the well-known min max game [12],[26]:

$$\min_G \max_D \mathcal{L}_{GAN}(D, G) \quad (1)$$

$$\mathcal{L}_{GAN(D,G)} = E_{(x,s)}[\log(x, s)] + E_{(s \sim p_{data}(s))}[\log(1 - D(s, G(s)))] \quad (2)$$

3.2 Embedding edge maps

In order to generate photo-realistic visually appealing images containing fine details, we provide an edge map (fig 2.1) of the real image to the generator, allowing it to learn the conditional distribution of real images given semantic maps and edge maps, i.e.:

$$\mathcal{L}_{GAN(D,G,e)} = E_{(x,s)}[\log(x, s)] + E_{((s,e) \sim p_{data}(s,e))}[\log(1 - D(s, G(s, e)))] \quad (3)$$

Note, the edge map is computed only during training while we present the generator with semantic maps and real images, so DNED only learns the distribution of real image edge maps. Since this paper addresses the problem of CG2real, the edge map can be estimated from the simulated image as well, thus is available at test time. During training, given an example image x_i , we can estimate its edge map by the well-known spatial Laplacian operator [13],[8]. This edge map is concatenated to the semantic label map and both are given as priors to the generator for adversarial training of the fake image f_i vs. the real image x_i . To allow a stable training we begin by training with the Laplacian operator itself, and after stabilization we replaced it with DNED and trained jointly the GAN and DNED.

Increasing the resolution of the image might be challenging for GAN training. In other methods the discriminator needs a large receptive field [17],[27],[29],[20], requiring a deeper network or larger convolution kernels. Using a deeper network is prone to overfitting and in the case of GAN training, and might cause training to be unstable. This challenge is usually addressed by the multi-scale approach [11],[8],[15],[19],[38]. Since the DNED embed high frequency details of images our architecture performs very well on higher resolution images. Our original generated images were of size [512x256]. We have successfully trained our model to generate images of size [768x384], i.e. 1.5 times larger in each dimension without changing the model while using a single discriminator (see 3.2). The loss function is therefore reduces to:

$$\mathcal{L}_{FM_s}(D, G, e) = \frac{1}{N} E_{(x,s,e) \sim p_{data}(s,x,e)} \mathcal{L}_1(D(s, x) - D(s, G(s, e))) \quad (4)$$

We showed that generating high quality images when using a single discriminator is feasible and training is stable. We provide comparison using our method with multi-scale discriminator 3.2, in that case the loss can be expanded to:

$$\mathcal{L}_{FM_m}^k := \mathcal{L}_{FM_m}^k(D_k, G, e) = \sum_{i=1}^T \frac{1}{N_i} E_{(x,s,e) \sim p_{data}(s,x,e)} \mathcal{L}_1(D_k^i(s, x) - D_k^i(s, G(s, e))) \quad (5)$$



Figure 3: comparison of 768x384 pix images generated by pix2pixHD (Left) and our model (Right). Our model can generate lower level details in the image, thus improving its photo-realism. This figure provides an example comparing (768x384 pix) resolution images of pix2pixHD (left side) compared to our model (right).

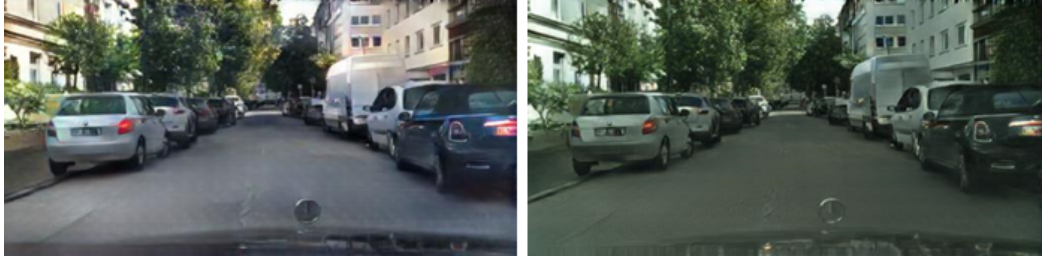


Figure 4: Comparison of generated test images, when network was trained with a single discriminator and a multi-scale discriminator. The left image is generated when the generator was trained with a single discriminator, while the right image while using a multi-scale discriminator.

The DNED architecture is a modified version of HED [37]. In HED, they are generating several sized versions of the edge map, each having a different receptive field. The purpose is to create an ensemble of edge maps, each allowing different level of details in the image. When superimposing all, the resulting edge map will have coarse-to-fine level of details in the generated edge map image. By changing the weights of that ensemble, we can generate the desired variability in the generated edge map, thus allowing us to generate diverse versions of the output. To conclude, the loss function for training the DNED is:

$$\mathcal{L}_{DNED} := \mathcal{L}_{DNED}(E(x)) = \sum_{i=1}^N a_i * BCE(d_i(x), E(x)) \quad (6)$$

Where: $d_i(x)$, $i = 0 : 5$ is the i^{th} side output of a single scale, $E(x)$ is the classic edge map generated by the spatial Laplacian operator, BCE is the binary cross entropy loss. $N = 6$ in our case. a_i is the contribution of the i^{th} scale to the ensemble.



Figure 5: By using edge maps, the model learns to separate objects of the same semantics. The most dominant example is buildings. Unlike cars, pedestrians or bicycle riders, that are separable using the instance map, buildings are not. The semantic label provides the pixels in which the building exists. Considering the fact that a scene of adjacent buildings is somewhat common, the ability to separate them is of high value. Left - the label map. Middle - generated image by [35]. Right - our generated image. Our model can generate unique adjacent buildings from the semantic label maps of better quality compared to [35].

In addition, following [9],[10],[18],[42] we are using the perceptual loss for improved visual performance, rather than L_1 loss.

$$\mathcal{L}_{percep} := \mathcal{L}_{percep}(x, G(s, e)) = \frac{1}{P} \sum_{i=1}^P \mathcal{L}_1(FL_{VGG_i}(x) - FL_{VGG_i}(G(s, e))) \quad (7)$$

Where, P is the number of slices from a pre-trained VGG network and FL_{VGG_i} are the features extracted by the VGG network from the i^{th} layer of the real and generated images respectively.

To conclude, our overall objective for generating photo-realistic, diverse images in the CG2real setting is to minimize $L_{CG2real}$:

$$L_{CG2real} = \min_G \max_{D_k, k=1:l_m} \sum_{l=1}^{l_m} \mathcal{L}_{GAN}(D_k, G, e) + \lambda_1 \sum_{l=1}^{l_m} \mathcal{L}_{FM_m}^k + \lambda_2 \mathcal{L}_{percep} + \lambda_3 \mathcal{L}_{NNED} \quad (8)$$

When $l_m = 1$ is used for the single scale discriminator and $l_m = 3$ for the multi scale one. see our results for the final image generation model (fig 3.2).



Figure 6: previous work test images [35] (Top) compared to our model test images (Bottom). The images generated by our model contain low level details, allowing the desired photo-realism

3.3 Videos generation

Given our CG2real scheme, we are generating two consecutive images, and then estimate two flow maps. The first flow map is between x_i, x_{i+1} , where x_i and x_{i+1} are two consecutive real images. The second flow map is between $G(s_i, e_i), G(s_{i+1}, e_{i+1})$, where $G(s_i, e_i)$ and $G(s_{i+1}, e_{i+1})$ are two consecutive generated (fake) images. Note that the generation of $G(s_i, e_i), G(s_{i+1}, e_{i+1})$ is done independently, meaning we apply our CG2real method twice, without any modifications.

To conclude we learn temporally coherent sequence of images, using this simple loss:

$$\mathcal{L}_{flow} = \mathcal{L}_1(\mathcal{F}_{real}, \mathcal{F}_{fake}) \quad (9)$$

Where $\mathcal{F}_{real} = \mathcal{F}(x_i, x_{i+1})$, $\mathcal{F}_{fake} = \mathcal{F}(G(s_i, e_i), G(s_{i+1}, e_{i+1}))$ and $\mathcal{F}(\cdot)$ is the optical flow operator. This formulation eliminates the need of using a sequential generator as in [34], allowing us not only using our image generation model twice, which adds more constraints to the video generation scheme, but also avoid accumulation errors arising from positive feedback from feeding a generated image to the generator, as can be seen in figure 3.3.

By adding L_{flow} to the $L_{CG2real}$ loss, the network learns to generate $G(s_{i+1}, e_{i+1})$ taking the flow maps into account, thus generating temporally coherent images.

$$\mathcal{L}_{videogen} = \mathcal{L}_{flow} + \mathcal{L}_{CG2real} \quad (10)$$

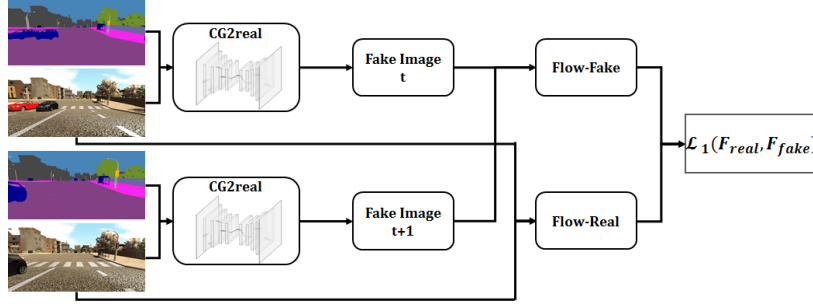


Figure 7: block diagram of the video generation model. Two identical CG2real models generate two consecutive fake images, namely Fake image (t) and Fake image (t+1). The two consecutive fake images are fed to the flow-fake estimator, while two consecutive real images are fed to the flow-real estimator. Both real and fake flow maps are trained using $L_1(F_{real}, F_{fake})$ loss. This enables each of the generators of the CG2real models to learn the required coherency for generating photo-realistic videos.

This way we train two instances of CG2real models and allow the temporal coherence between two consecutive generated images as depicted in 3.3.



Figure 8: Comparison of video generation. Left column - real images. Middle column - images generated by vid2vid [34]. Right column - images generated by our video generation model. The generated images by our model are temporally coherent and visually appealing. The main objective of the video generation model is to enable generating non flickering images by giving objects in consecutive images the same color and texture, i.e. sample from the same area in the latent spaces.

4 Results

Our goal is to generate photo-realistic images. In (fig 3.2) we can find some examples from the CG2real image synthesis task, and in (fig 3.3) present consecutive images depicting the video to video synthesis. We use the same evaluation methods as used by previous image to image works ,e.g. pix2pix [17] , pix2pixHD [35] and others. The evaluation process consist of performing semantic segmentation with a pre-trained seamntic segmentation network [39] on the synthesized images our model produced, then calculating the semantic pixel accuracy and the mean intersection over union (mIoU) over the classes in the dataset. As shown in tables 1, 2 bellow, our network outperforms previous works. The ground-truth results are the pixel accuracy and mIoU when performing the same semantic segmentation with the real images (Oracle).

Furthermore, to evaluate the image generation quality, we used another metric to evaluate distances between datasets called FID (Fréchet Inception Distance) [14],[1]. It is a very common metric for generative models as it correlates well with the visual quality of generated samples [34]. FID calculates the distance between two multivariate Gaussians real and generated respectively; where $X_r \sim N(\mu_r, \Sigma_r)$ and $X_g \sim N(\mu_g, \Sigma_g)$ are the 2048-dimensional activations of the Inception-v3 pool3 layer[30], and $FID = \|\mu_r - \mu_g\|^2 + Tr(\Sigma_r + \Sigma_g - 2(\Sigma_r \Sigma_g)^{1/2})$ is the score for image distributions X_r and X_g . Lower FID score is better, meaning higher similarity between real and generated samples.

Cityscapes	Pix2pix	Pix2pixHD	Ours	Oracle
Pixel accuracy [%]	0.7279	0.81	0.83	0.86
Mean IoU [%]	0.5324	0.67	0.69	0.701

Table 1: semantic segmentation results on the cityscapes [7] validation set

Synthia	Pix2pix	Pix2pixHD	Ours	Oracle
Pixel accuracy [%]	0.54	0.79944	0.860753	0.913132
Mean IoU [%]	0.36	0.55955	0.740040	0.8419

Table 2: semantic segmentation results on the Synthia [24] dataset

FID,FVD	Pix2pix	Pix2pixHD	Vid2vid	Ours-img	Ours-vid
FID	116.69	71.21	154.36	69.25	69.81
FVD	-	-	0.706	-	0.326

Table 3: FID and FVD metric comparisson between pix2pix, pix2pixHD vid2vid and Ours.

As can be seen in tables 1, 2, pix2pixHD’s results are better than pix2pix for pixel accuracy and mIoU. Our results are better than pix2pixHD, and almost meet the oracle’s results on both Synthia [24] and cityscapes [7]. In table 3, we compare the FID score for all the four image generation models w.r.t the Oracle. Video to video adds a temporal consistency constrain in addition to the image to image process, therefore the model might suffer from image quality degradation. Vid2vid uses pix2pixHD as its image generation model but in the process suffers from degradation in the image quality. Our video generation which uses our CG2real model although encountering some image quality loss, still outperforms pix2pixHD on FID. The FID score of vid2vid w.r.t. its image generation model, i.e. pix2pixHD degrades more than twice (71.21 -> 154.36), while nearly suffers degraded performance (69.25 -> 69.81).

Our video generation evalutaion method is evaluated according to a recent work by [32] named Fréchet Video Distance (FVD). FVD is a metric for evaluating video generation models and it uses a version of FID, with a modification to evaluate video generation. we calculated the FVD score for our generated video w.r.t. the Oracle (real video) and did the same for vid2vid [34]. Our FVD score on the video test set is 0.326 while vid2vid’s [34] is 0.706 meaning our is more than twice similar to the oracle.

5 Summary

We present a CG2real conditional image generation as well as a conditional video synthesis. We offer to use a network learning the distribution of edge maps for real images and integrate it into a generator (DNED). We were able to generate high level details images thus enabling better photo-realism. Using the DNED enable generating diverse yet photo-realistic realizations of the same desired scene without using instance maps. As for video generation, we offer a new scheme that utilizes flow maps allowing better temporal coherence in a videos. We compared our model to recent works and found that it outperforms both current quantitative results and more importantly generates appealing images. Furthermore, our video generation model generates temporally coherent, elegant videos.

References

- [1] Jonas Adler and Sebastian Lunz. Banach wasserstein gan. In S. Bengio, H. Wallach, H. Larochelle, K. Grauman, N. Cesa-Bianchi, and R. Garnett, editors, *Advances in Neural Information Processing Systems 31*, pages 6754–6763. Curran Associates, Inc., 2018.
- [2] Martin Arjovsky, Soumith Chintala, and Léon Bottou. Wasserstein gan. *arXiv preprint arXiv:1701.07875*, 2017.
- [3] Xue Bai, Jue Wang, David Simons, and Guillermo Sapiro. Video snapcut: Robust video object cutout using localized classifiers. In *ACM SIGGRAPH 2009 Papers*, SIGGRAPH '09, pages 70:1–70:11, New York, NY, USA, 2009. ACM.
- [4] Yochai Blau and Tomer Michaeli. The perception-distortion tradeoff. *2018 IEEE/CVF Conference on Computer Vision and Pattern Recognition*, Jun 2018.
- [5] Qifeng Chen and Vladlen Koltun. Photographic image synthesis with cascaded refinement networks. In *Proceedings of the IEEE International Conference on Computer Vision*, pages 1511–1520, 2017.
- [6] Jack Collins, David Howard, and Jürgen Leitner. Quantifying the reality gap in robotic manipulation tasks. *arXiv preprint arXiv:1811.01484*, 2018.
- [7] Marius Cordts, Mohamed Omran, Sebastian Ramos, Timo Rehfeld, Markus Enzweiler, Rodrigo Benenson, Uwe Franke, Stefan Roth, and Bernt Schiele. The cityscapes dataset for semantic urban scene understanding. In *Proc. of the IEEE Conference on Computer Vision and Pattern Recognition (CVPR)*, 2016.
- [8] Emily Denton, Soumith Chintala, Arthur Szlam, and Rob Fergus. Deep generative image models using a laplacian pyramid of adversarial networks, 2015.
- [9] Alexey Dosovitskiy and Thomas Brox. Generating images with perceptual similarity metrics based on deep networks, 2016.
- [10] Leon A Gatys, Alexander S Ecker, and Matthias Bethge. Image style transfer using convolutional neural networks. In *Proceedings of the IEEE conference on computer vision and pattern recognition*, pages 2414–2423, 2016.
- [11] Golnaz Ghiasi and Charless C. Fowlkes. Laplacian pyramid reconstruction and refinement for semantic segmentation. *Lecture Notes in Computer Science*, page 519–534, 2016.
- [12] Ian Goodfellow, Jean Pouget-Abadie, Mehdi Mirza, Bing Xu, David Warde-Farley, Sherjil Ozair, Aaron Courville, and Yoshua Bengio. Generative adversarial nets. In *Advances in neural information processing systems*, pages 2672–2680, 2014.
- [13] Stephen Guattery and Gary L. Miller. Graph embedding and laplacian eigenvalues. *SIAM J. Matrix Anal. Appl.*, 21(3):703–723, 2000.
- [14] Martin Heusel, Hubert Ramsauer, Thomas Unterthiner, Bernhard Nessler, and Sepp Hochreiter. Gans trained by a two time-scale update rule converge to a local nash equilibrium. In *Advances in Neural Information Processing Systems*, pages 6626–6637, 2017.
- [15] Xun Huang, Yixuan Li, Omid Poursaeed, John Hopcroft, and Serge Belongie. Stacked generative adversarial networks. *2017 IEEE Conference on Computer Vision and Pattern Recognition (CVPR)*, Jul 2017.
- [16] Eddy Ilg, Nikolaus Mayer, Tonmoy Saikia, Margret Keuper, Alexey Dosovitskiy, and Thomas Brox. FlowNet 2.0: Evolution of optical flow estimation with deep networks. *2017 IEEE Conference on Computer Vision and Pattern Recognition (CVPR)*, Jul 2017.
- [17] Phillip Isola, Jun-Yan Zhu, Tinghui Zhou, and Alexei A Efros. Image-to-image translation with conditional adversarial networks. In *Proceedings of the IEEE conference on computer vision and pattern recognition*, pages 1125–1134, 2017.

- [18] Justin Johnson, Alexandre Alahi, and Li Fei-Fei. Perceptual losses for real-time style transfer and super-resolution. *Lecture Notes in Computer Science*, page 694–711, 2016.
- [19] Tero Karras, Timo Aila, Samuli Laine, and Jaakko Lehtinen. Progressive growing of gans for improved quality, stability, and variation, 2017.
- [20] Wenjie Luo, Yujia Li, Raquel Urtasun, and Richard Zemel. Understanding the effective receptive field in deep convolutional neural networks. In *Advances in neural information processing systems*, pages 4898–4906, 2016.
- [21] Mehdi Mirza and Simon Osindero. Conditional generative adversarial nets, 2014.
- [22] Augustus Odena, Christopher Olah, and Jonathon Shlens. Conditional image synthesis with auxiliary classifier gans. In *Proceedings of the 34th International Conference on Machine Learning-Volume 70*, pages 2642–2651. JMLR. org, 2017.
- [23] Alec Radford, Luke Metz, and Soumith Chintala. Unsupervised representation learning with deep convolutional generative adversarial networks, 2015.
- [24] German Ros, Laura Sellart, Joanna Materzynska, David Vazquez, and Antonio M. Lopez. The synthia dataset: A large collection of synthetic images for semantic segmentation of urban scenes. In *The IEEE Conference on Computer Vision and Pattern Recognition (CVPR)*, June 2016.
- [25] Masaki Saito, Eiichi Matsumoto, and Shunta Saito. Temporal generative adversarial nets with singular value clipping. *2017 IEEE International Conference on Computer Vision (ICCV)*, Oct 2017.
- [26] Tim Salimans, Ian Goodfellow, Wojciech Zaremba, Vicki Cheung, Alec Radford, and Xi Chen. Improved techniques for training gans. In *Advances in neural information processing systems*, pages 2234–2242, 2016.
- [27] George Seif and Dimitrios Androutsos. Large receptive field networks for high-scale image super-resolution. In *Proceedings of the IEEE Conference on Computer Vision and Pattern Recognition Workshops*, pages 763–772, 2018.
- [28] Oded Shahrar, Alon Faktor, and Michal Irani. Super-resolution from a single video. In *CVPR*, 2011.
- [29] Karen Simonyan and Andrew Zisserman. Very deep convolutional networks for large-scale image recognition. *arXiv preprint arXiv:1409.1556*, 2014.
- [30] Christian Szegedy, Vincent Vanhoucke, Sergey Ioffe, Jon Shlens, and Zbigniew Wojna. Rethinking the inception architecture for computer vision. *2016 IEEE Conference on Computer Vision and Pattern Recognition (CVPR)*, Jun 2016.
- [31] Sergey Tulyakov, Ming-Yu Liu, Xiaodong Yang, and Jan Kautz. Mocogan: Decomposing motion and content for video generation. *2018 IEEE/CVF Conference on Computer Vision and Pattern Recognition*, Jun 2018.
- [32] Thomas Unterthiner, Sjoerd van Steenkiste, Karol Kurach, Raphael Marinier, Marcin Michalski, and Sylvain Gelly. Towards accurate generative models of video: A new metric & challenges. *arXiv preprint arXiv:1812.01717*, 2018.
- [33] Carl Vondrick, Hamed Pirsiavash, and Antonio Torralba. Generating videos with scene dynamics, 2016.
- [34] Ting-Chun Wang, Ming-Yu Liu, Jun-Yan Zhu, Guilin Liu, Andrew Tao, Jan Kautz, and Bryan Catanzaro. Video-to-video synthesis, 2018.
- [35] Ting-Chun Wang, Ming-Yu Liu, Jun-Yan Zhu, Andrew Tao, Jan Kautz, and Bryan Catanzaro. High-resolution image synthesis and semantic manipulation with conditional gans. In *Proceedings of the IEEE Conference on Computer Vision and Pattern Recognition*, 2018.

- [36] Yonatan Wexler, Eli Shechtman, and Michal Irani. Space-time video completion. In *Proceedings of the 2004 IEEE Computer Society Conference on Computer Vision and Pattern Recognition, 2004. CVPR 2004.*, volume 1, pages I–I. IEEE, 2004.
- [37] Saining Xie and Zhuowen Tu. Holistically-nested edge detection. *International Journal of Computer Vision*, 125(1-3):3–18, Mar 2017.
- [38] Han Zhang, Tao Xu, and Hongsheng Li. Stackgan: Text to photo-realistic image synthesis with stacked generative adversarial networks. *2017 IEEE International Conference on Computer Vision (ICCV)*, Oct 2017.
- [39] Hengshuang Zhao, Jianping Shi, Xiaojuan Qi, Xiaogang Wang, and Jiaya Jia. Pyramid scene parsing network. *2017 IEEE Conference on Computer Vision and Pattern Recognition (CVPR)*, Jul 2017.
- [40] Junbo Zhao, Michael Mathieu, and Yann LeCun. Energy-based generative adversarial network, 2016.
- [41] Jun-Yan Zhu, Philipp Krähenbühl, Eli Shechtman, and Alexei A. Efros. Generative visual manipulation on the natural image manifold. *Lecture Notes in Computer Science*, page 597–613, 2016.
- [42] Jun-Yan Zhu, Richard Zhang, Deepak Pathak, Trevor Darrell, Alexei A Efros, Oliver Wang, and Eli Shechtman. Toward multimodal image-to-image translation. In *Advances in Neural Information Processing Systems*, pages 465–476, 2017.